

# Comparison of the periodic slab approach with the finite cluster ansatz for metal-organic interfaces at the example of PTCDA on Ag(110)

Jaita Banerjee,<sup>1,\*</sup> Stefan Behnle,<sup>1</sup> Martin C. E. Galbraith,<sup>2,†</sup> Hans-Georg Mack,<sup>1</sup>  
Volker Settels,<sup>3,‡</sup> Bernd Engels,<sup>3</sup> Ralf Tonner,<sup>2,§</sup> and Reinhold F. Fink<sup>1,¶</sup>

<sup>1</sup>*Institut für Physikalische und Theoretische Chemie,  
Auf der Morgenstelle 18, Universität Tübingen, 72076 Tübingen, Germany*

<sup>2</sup>*Fachbereich Chemie, Philipps-Universität Marburg,  
Hans-Meerwein-Str. 4, D-35032 Marburg, Germany*

<sup>3</sup>*Institut für Physikalische und Theoretische Chemie,  
Universität Würzburg, Emil-Fischer-Str. 42, 97074 Würzburg, Germany.*

(Dated: February 18, 2022)

## Abstract

We present a comparative study of metal-organic interface properties obtained from dispersion corrected density functional theory calculations based on two different approaches: the periodic slab supercell technique and cluster models with 18 to 290 Ag atoms. Fermi smearing and fixing of cluster borders are required to make the cluster calculation feasible and realistic. The considered adsorption structure and energy of a PTCDA molecule on the Ag(110) surface is not well reproduced with clusters containing only two metallic layers. However, clusters with four layers of silver atoms and sufficient lateral extension reproduce the adsorbate structure within 0.02 Å and adsorption energies within 10% of the slab result. A consideration of the computational effort shows that the cluster approach is a competitive alternative to methods using periodic boundary conditions and of particular interest for research at surface defects and other systems that do not show periodic symmetry.

---

\* Present address: University and Institute of Advanced Research, Koba Institutional Area, Gandhinagar - 382007, Gujarat, India

† Present address: Max-Born Institute, Berlin Germany.

‡ Present address: BASF SE GNC/M - B001 Ludwigshafen Germany

§ tonner@chemie.uni-marburg.de

¶ reinhold.fink@uni-tuebingen.de

## I. INTRODUCTION

Interfaces formed when large organic  $\pi$ -conjugate molecules adsorb on metallic substrates represent crucial functional parts in a variety of nano and micro, electronic and optoelectronic devices, such as organic solar cells, organic light emitting diodes, organic field-effect transistors and other devices [1, 2]. The importance of these interfaces is that they are often essential for the generation, injection and transportation of charges in the device [3–5]. The bonding nature of the molecule to the surface is of particular interest as it affects these properties substantially [6, 7].

Several interesting studies of organic-metal interfaces are found in the literature, where the interactions of a variety of organic molecules (pentacene, perylene derivatives, phthalocyanines) have been studied on the low index planes of noble metals, namely Ag, Cu and Au [8–16]. In this paper we will restrict the discussion to the adsorption of Perylene-3,4,9,10-tetracarboxylic dianhydride (PTCDA) on the Ag(110) surface which is a prototype system as its adsorption characteristics have been very well studied [11, 12, 17–25]. Besides detailed information on the lateral orientation of the molecule upon the metal surface, x-ray standing wave (XSW) measurements provide accurate information about the distance between the individual atoms of the molecule from the surface [20, 24].

Density Functional Theory (DFT) [26, 27] is one of the most widely used tools for studying metals and metal surfaces due to its ability for providing a realistic description of the electronic structure of these systems. Unfortunately, local [28–30] or semi-local [31, 32] density functionals are not able to properly reproduce London dispersion interactions which are significantly affecting the structure of aggregates in general and thus also of metal adsorbate systems. To address this issue, several techniques have been designed [25, 33–40]. It was shown that the inclusion of dispersion corrections is crucial in the treatment of large  $\pi$ -systems on noble metal substrates [22, 25, 41–44]. Of these, the DFT-D3(BJ) empirical scheme developed by Grimme *et al.* [40] performs remarkably well in predicting the structure and adsorption energy of organic molecules on surfaces [12, 24, 45].

The most common theoretical approach to metal-organic interfaces is the periodic slab-supercell approach (see e.g. [44–47]) where the adsorbate is placed on the surface and periodic boundary conditions are applied. The resulting system replicates a physical surface-adsorbate system by an infinite stack of equally spaced metallic slabs. The slabs are rather

thin periodic metallic surfaces with molecules adsorbed in a two dimensional periodic arrangement. Tuning the distance between two adjacent periodic images allows to control the interaction between neighbouring slabs while modulating the size of the surface unit cell makes it possible to control the interaction between neighbouring adsorbate molecules.

As an alternative to the slab model, the cluster approach can be employed by cutting several metal atoms out of the surface and placing a molecule upon it. This means that the metal surface is represented by a brick of atoms in the vacuum [48]. This model has also been used frequently, e.g. for adsorbates on silver [22, 41, 43] and other metals [41, 49–53]. Generally it is significantly more difficult to design a proper cluster than to set up a periodic slab calculation as it is not clear how the lateral extension of the cluster and the corresponding borders influence the metal adsorbate properties. Another challenge for the cluster approach is to find appropriate orbital occupations. Due to small energy gaps it is generally unclear which orbitals should be occupied and which spin multiplicity is appropriate to describe the electronic structure of the metal surface [49, 51].

However, cluster calculations have some advantages: They are usually conducted with quantum chemical program packages using local Gaussian basis sets whereas continuous plane wave basis sets are most commonly employed for the slab model. For a given system the number of local basis functions required to expand the electronic wavefunctions is generally significantly smaller than the corresponding number of plane wave functions. The latter allow for very efficient evaluation of the Coulombic electron repulsion energy [54] which overcompensated the disadvantage of dealing with a higher number of basis functions for a long time. However, efficient implementations of DFT in Quantum Chemical program packages are available [55, 56]. These make use of the local nature of the basis functions and thus may turn the situation. Furthermore, the cluster approach is applicable to charged adsorbates [50] as well as other non-periodic systems and – in principle – it allows to apply accurate wave function based methods.

The motive of this work is to investigate whether structural and energetic properties of an adsorbate upon a metal surface converge to the results of a corresponding slab model by systematically increasing the cluster size. This comparison requires that the atomic and electronic structure of the metal is set up in the same way. The latter is achieved in our approach by employing the same structure at the cluster border and by using a pseudo Fermi [57] type occupation of the discrete orbitals. Basis set convergence is investigated as well as

the performance of different dispersion correction schemes.

The paper is organised as follows; in section II the computational details of the two approaches are discussed. In section III, we present the results obtained from the slab-supercell calculations and the cluster calculations, and a comparison between them. In section IV we summarise the work and discuss how the cluster ansatz may be improved and employed in future work.

## II. METHODS

### A. Structural Information

All calculations employed DFT using the generalised gradient approximation (GGA) Perdew-Burke-Ernzerhof (PBE) functional [32]. Three types of dispersion schemes were used: (i) without applying any dispersion correction (noD), (ii) applying the D2 [37] correction and (iii) the D3(BJ) [39, 40] correction which uses the rational damping of the dispersion contribution to finite values for small inter atomic distances as proposed by Becke and Johnson [58].

As described below, the slab-supercell approach requires only information of the bulk structure while our cluster approach needs also the relaxation pattern of the metal atoms near to the surface. This structural information was obtained with the Vienna Ab Initio Simulation Package (VASP) code which was also employed for the slab-supercell calculations. All VASP calculations were performed using plane wave basis sets and the projector augmented wave technique for treating core electrons efficiently [59–62]. The energy cut-off was set to 340 eV as this was found to be sufficient to converge the bulk lattice constant within  $< 1$  %. For further details see supporting information of Ref. [45]. The Methfessel-Paxton second order smearing technique [63] with a width of 0.2 eV was used. For the determination of the bulk structure, the Brillouin zone was sampled with a Monkhorst-Pack [64] distribution of  $11 \times 11 \times 11$   $\mathbf{k}$ -point mesh.

### B. Slab-supercell Approach

All slab-supercell calculations were performed with a rectangular  $\begin{pmatrix} 3 & 2 \\ -3 & 2 \end{pmatrix}$  surface unit cell. The slab was chosen to have four atomic layers, the two lowermost layers were kept

fixed at the bulk equilibrium structure obtained with the respective dispersion correction while the remaining two were relaxed. A sufficient vacuum separation of 20 Å was used for all calculations and the Brillouin zone was sampled with a  $3 \times 3 \times 1$   $\mathbf{k}$ -mesh. The nearest neighbour Ag-Ag distances resulting from the structural optimisation of the plain slabs are collected in Tab. I.

The adsorbate system was obtained by placing a PTCDA molecule on the Ag(110) surface in the experimentally determined lateral position [24, 65, 66] where the acyl and anhydride oxygen atoms are located silver atoms (atop sites) while the perylene core is located between two Ag rows.

The adsorption energy of the molecule to the Ag(110) surface was obtained by

$$E_{\text{ads}} = E_{\text{PTCDA/Ag(110)}} - (E_{\text{Ag(110)}} + E_{\text{PTCDA}}), \quad (1)$$

where  $E_{\text{PTCDA/Ag(110)}}$  is the total energy of the system when a PTCDA molecule is placed on the Ag(110) surface.  $E_{\text{Ag(110)}}$  is the total energy of the bare Ag(110) surface and  $E_{\text{PTCDA}}$  is the total energy of a PTCDA molecule in a large box without inter-molecular interactions.

### C. Finite Cluster Approach.

#### 1. Constructing Ag(110) Clusters.

The Ag(110) “surface” clusters were constructed from the optimised bare Ag(110) slab-supercell structures at the PBE-noD, -D2 and -D3(BJ) level (see Tab. I for the respective structural parameters). They contain two or four layers of Ag atoms along the (110) direction. A layer consisting of  $n$  atoms in the  $(1\bar{1}0)$  and  $m$  atoms in the  $(001)$  direction is designated as  $(n \times m)$ . All clusters are constructed such that the uppermost (first) layer of  $(n \times m)$  Ag atoms is followed by a larger second  $((n+1) \times (m+1))$  layer. Thus, the Ag-atoms contacting the adsorbate are relatively well embedded by the second layer atoms. This construction pattern avoids “naked” atoms at the surface and provides rather stable cluster surfaces. The third and fourth layers (if present) contain  $(n \times m)$  and  $((n-1) \times (m-1))$  Ag atoms.

The smallest cluster, Ag32, has two atomic layers with a  $(3 \times 4)$  top layer, and consists of 32 atoms. The second cluster of 50 atoms consists of a  $(5 \times 4)$  top layer and has also two

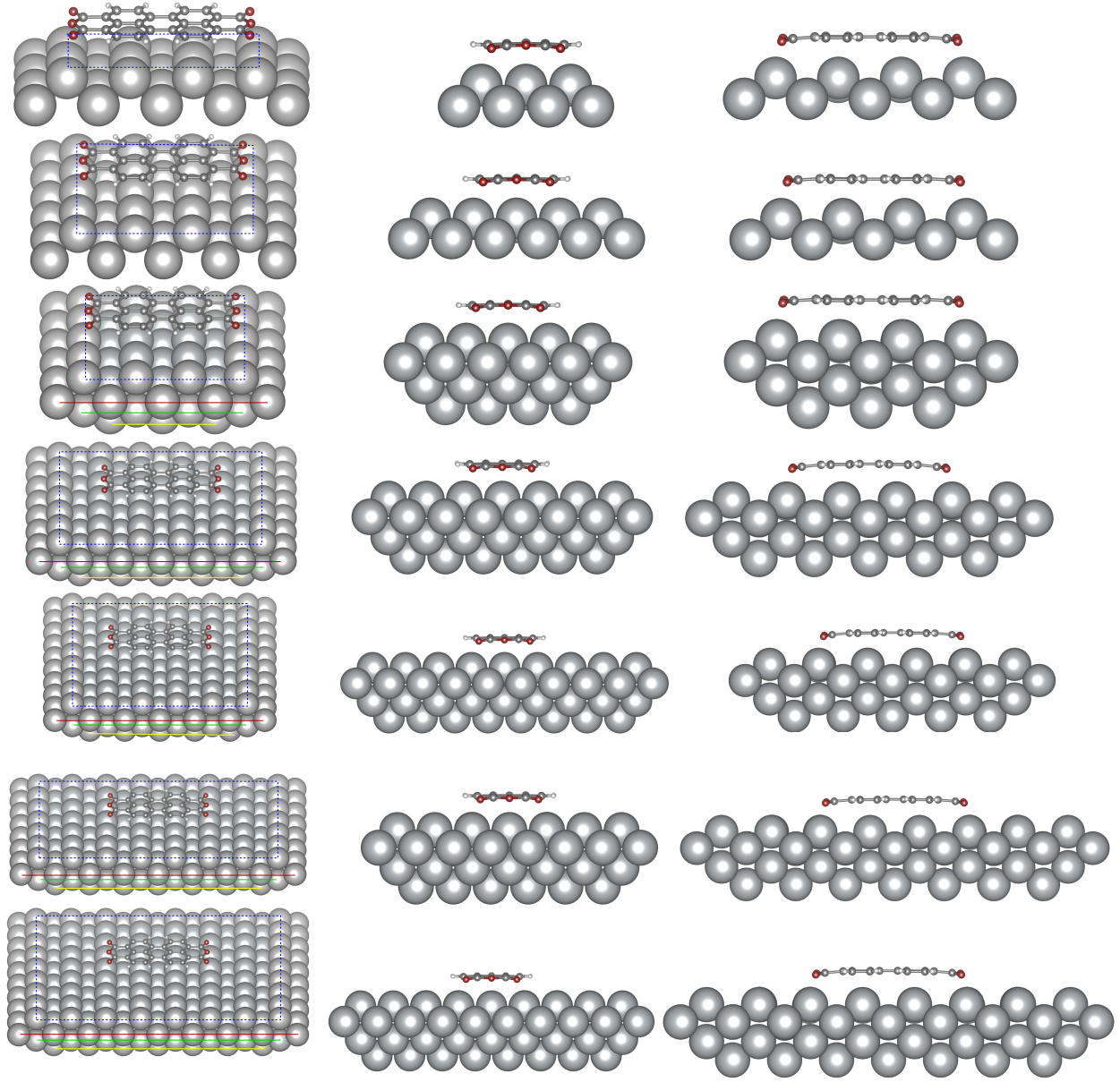


FIG. 1. Top to bottom: PTCDA on Ag(110) clusters consisting of 32, 50, 82, 170, 218, 226 and 290 atoms. Column 1: Initial configuration of PTCDA on the Ag(110) clusters. The blue rectangles border the topmost surface layer, the red, green and yellow lines is a guide to denote the 2nd, 3rd and 4th layers in all clusters except the 2 layered 32 and 50 atom clusters. Column 2 and Column 3 shows the side view along the molecular short axis and long axis respectively, of exemplary optimized structures. The molecule shows significant bending along the long axis for the larger clusters, starting from the 170 atom Ag(110) cluster.

layers. The other clusters all contain four layers with the following top layers: Ag82 ( $5 \times 4$ ), Ag170 ( $7 \times 6$ ), Ag218 ( $9 \times 6$ ), Ag226 ( $7 \times 8$ ), Ag290 ( $9 \times 8$ ).

For the clusters with two atomic layers, the lowermost layer was kept fixed, while the two lowermost layers were fixed for the four layer clusters just as in the periodic slab calculations. We adopt two schemes for fixing the border atoms of the first and the second top layers, which we refer to as fix12 - when the border atoms of both the top and the second layers are kept fixed and fix2 - when only the border atoms of the second layer are kept fixed.

## 2. Calculation details.

All cluster calculations were performed with the program package TURBOMOLE [67–69] employing the resolution of the identity (RI) method [55, 70, 71] and the multipole accelerated RI-J (MARI-J) approximation [56] which are known to speed up calculations without introducing significant errors. We used the def-SV(P) [72], def2-TZVP [73] and the def2-QZVP [73] basis sets with the corresponding auxiliary (RI) basis sets [55, 74] and ecp-28 effective core potentials for the silver atoms [75]. We employed the m3 grid as implemented in TURBOMOLE [55] to evaluate the energy expression and exploited the  $C_{2v}$  symmetry of the systems. A rather large damping parameter [76] in the range between 3.7 and 1.05 had to be used in order to guarantee convergence of the self consistent field (SCF) iterations. A total energy convergence criterion of  $1 \times 10^{-5} E_h$ , a Cartesian gradient norm criterion of  $1 \times 10^{-4}$  au and an SCF convergence criterion of  $1 \times 10^{-6}$  (see Ref. [76] for details on these parameters) was sufficient to converge structural parameters to 0.01 Å and adsorption energies to 0.01 eV. Further details are given in the supporting information of this article. The cluster computations were carried out using standard workstations with 4 cores or cluster nodes with 8 cores and up to 64 GB RAM.

In a quantum chemical program such as TURBOMOLE it is common to occupy orbitals with integer numbers of electrons. This turned out to be rather impractical for the cluster calculations as the HOMO-LUMO gap becomes very small such that orbitals near this gap frequently change their occupation within the SCF or structure convergence iterations. We found a straightforward albeit computationally demanding solution by performing a pseudo Fermi [57] smearing of the occupation of the cluster orbitals where a constant electronic temperature of 300 K was chosen. This was incorporated in context with spin restricted

Kohn-Sham determinants. For the larger clusters, several orbitals had fractional occupation numbers in the range between 0.1 and 1.9 electrons even in the converged orbitals. As Fermi smearing spoils the convergence acceleration method implemented in TURBOMOLE, in many cases several hundred SCF iterations were required to converge the electronic structure of a given cluster model. Nevertheless, the efficiency of the RI and MARI-J approximations allowed to conduct structural optimisations of even the largest clusters on our relatively simple computing resources within a few days. The wall clock time for the full structural optimisation of the PTCDA@Ag<sub>290</sub> system with PBE-D3(BJ) and the def2-TZVP basis set was in the order of 20 days.

#### D. Definition of Distances.

The distance of the atoms of an adsorbate can be determined experimentally with the XSW technique which provides structural information of all those atoms that give rise to a distinguishable signal in the X-ray photoelectron spectrum (XPS). XSW determines the distance between these atoms and the virtual plane of the relaxation-free uppermost layer of crystal atoms, i.e., the plane of the surface atoms if these did not relax from their bulk positions [45, 77]. According to the proposal of Woodruff [77] (see Fig. 2) we calculate the XSW distance of the atom  $A$  in the molecule from the slab or cluster structure as

$$d_A = (z_A - z_{\text{Ag}_n}) - (n - 1)\Delta z_{\text{bulk}}, \quad (2)$$

where  $z_A$  represents the vertical distance of the atom  $A$  from the surface,  $n$  is the number of Ag-layers in the cluster, and  $\Delta z_{\text{bulk}}$  is the distance obtained from periodic slab supercell calculations. In eq. (2) we rather use the theoretically optimised than the experimental value for  $\Delta z_{\text{bulk}}$  as the property of interest is actually the position of the molecule on the top layer. The position of this top layer is incorrectly described with the experimental  $\Delta z_{\text{bulk}}$  and this error increases with the number of layers in the slab or cluster model.



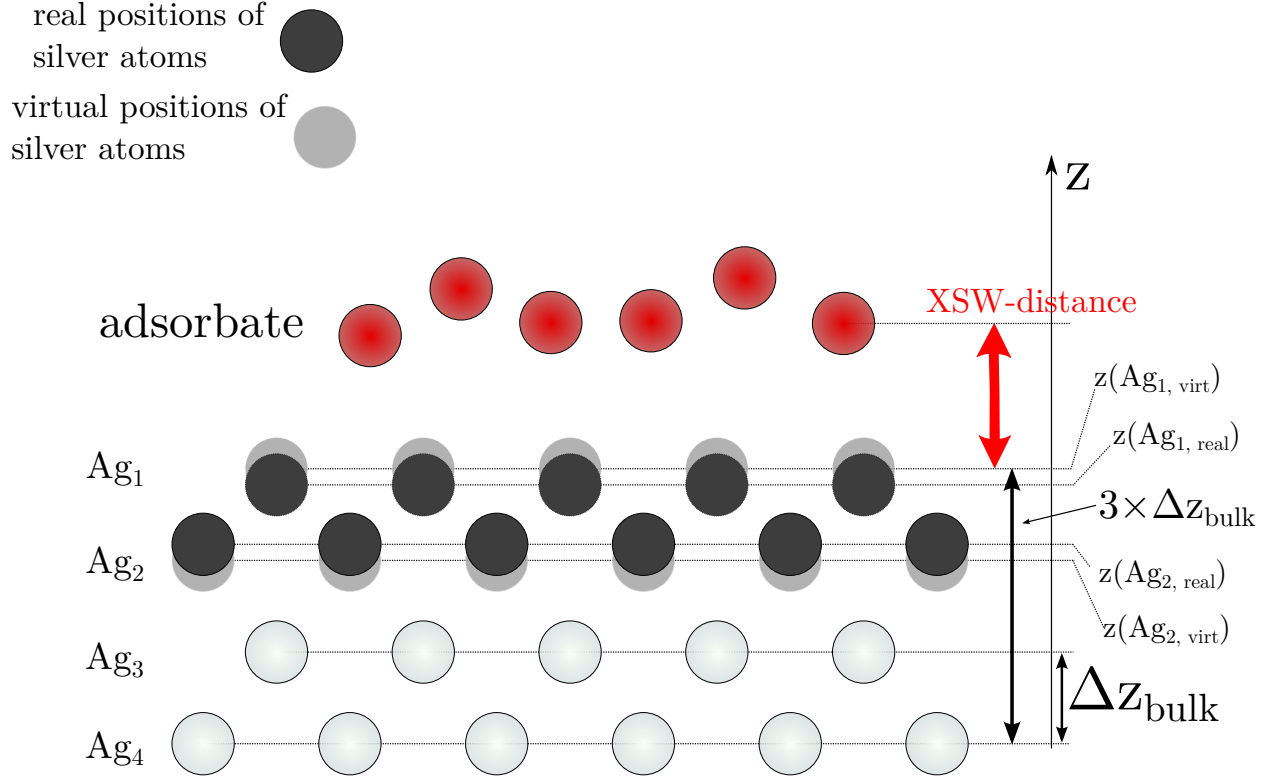


FIG. 2. XSW distances for four layer Ag(110) clusters. The relaxed (bulk) first and second layers are denoted by  $\text{Ag}_{1,\text{real}}$  ( $\text{Ag}_{1,\text{virt}}$ ) and  $\text{Ag}_{2,\text{real}}$  ( $\text{Ag}_{2,\text{virt}}$ ), respectively.  $\Delta z_{\text{bulk}}$  is the bulk interlayer separation.

TABLE I. Next neighbor Ag-Ag distances,  $r_{nm}$ , between Ag atoms in the  $n$ th and the  $m$ th layer for the free Ag(110) surface and vertical distances of the Ag layers as obtained with the slab calculations.  $\text{Ag}_n$  denotes an atom in the  $n$ th layer where  $n = 1$  is the topmost layer at the surface. All distances in Å. Numbers in brackets are the percentage relaxations of the vertical layer distances.

method	$r_{\text{Ag}_1-\text{Ag}_2}$	$r_{\text{Ag}_1-\text{Ag}_2}$	$r_{\text{Ag}_{\text{bulk}}-\text{Ag}_{\text{bulk}}}$	$z_{\text{Ag}_1} - z_{\text{Ag}_2}$	$z_{\text{Ag}_2} - z_{\text{Ag}_3}$	$\Delta z_{\text{bulk}}$
PBE	2.864	2.969	2.933	1.323 (−9.8 %)	1.537 (+4.8 %)	1.467
PBE-D2	2.847	3.026	2.921	1.306 (−10.6 %)	1.661 (+13.7 %)	1.461
PBE-D3(BJ)	2.836	2.928	2.880	1.350 (−6.3 %)	1.534 (+6.5 %)	1.440
expt. <sup>a</sup>			2.889		1.445	

<sup>a</sup> Ref. [78]

### III. RESULTS AND DISCUSSION

#### A. Bulk Distances

Tab. I shows the nearest neighbour and adjacent atomic layer distances of silver atoms as obtained in the slab calculations with the noD, D2, and D3(BJ) dispersion corrections as well as the experimental bulk distances. The nearest neighbour distance obtained with the D3(BJ) approach deviates only by  $-0.009 \text{ \AA}$  from the experimental value while the two other approaches overestimate the Ag-Ag distances by about  $0.03 \text{ \AA}$ .

All methods predict that the distance between the second and third layers is longer than the layer distance in the bulk,  $\Delta z_{bulk}$ , while the distance between the first and second layer atoms is smaller than that. LEED- $I(V)$  experiments of Nascimento *et al.* [79] as well as XSW data of Bauer *et al.* [12] and DFT calculations [79–81] indicate that the distance between the first and second atomic layer of silver is contracted by  $-7.5 \pm 3.0 \%$  while  $d_{Ag_2-Ag_3}$  is extended by  $2 \pm 5 \%$  with respect to the bulk interlayer distance  $\Delta z_{bulk} = 1.445 \text{ \AA}$ .

We note that this relaxation pattern is not observed in the D2 and D3(BJ) model. This is probably due to the repulsive part of the interaction energy that appears from the damping of the dispersion correction. Fig. 3 shows that this damping leads to artificial repulsive contributions to the total energy for the typical nearest neighbour silver-silver distance which are, thus, stretched if these dispersion corrections are applied.

#### B. Adsorbate Structures

In this section the convergence of the adsorbate structures is investigated with respect to (i) the dispersion scheme [noD, D2, D3(BJ)], (ii) the basis set [def-SV(P), def2-TZVP], (iii) fixing of border atoms [fix2, fix12], and (iv) the cluster size (32, 50, 82, 170, 218, 226 and 290 silver atoms). Most of these combinations were investigated and compared with the results of the slab-supercell calculations. As the  $Ag_{170}$  cluster with the fix12-scheme and the def2-TZVP basis set provides reasonably well converged results, we shall use this as a reference for the following comparisons. Further results are collected in the supporting information of this article.

The adsorption height of PTCDA above the Ag(110) surface is determined by the following XSW distances:  $C_{aromat}$  is the *average* distance of the 20 carbon atoms in the perylene

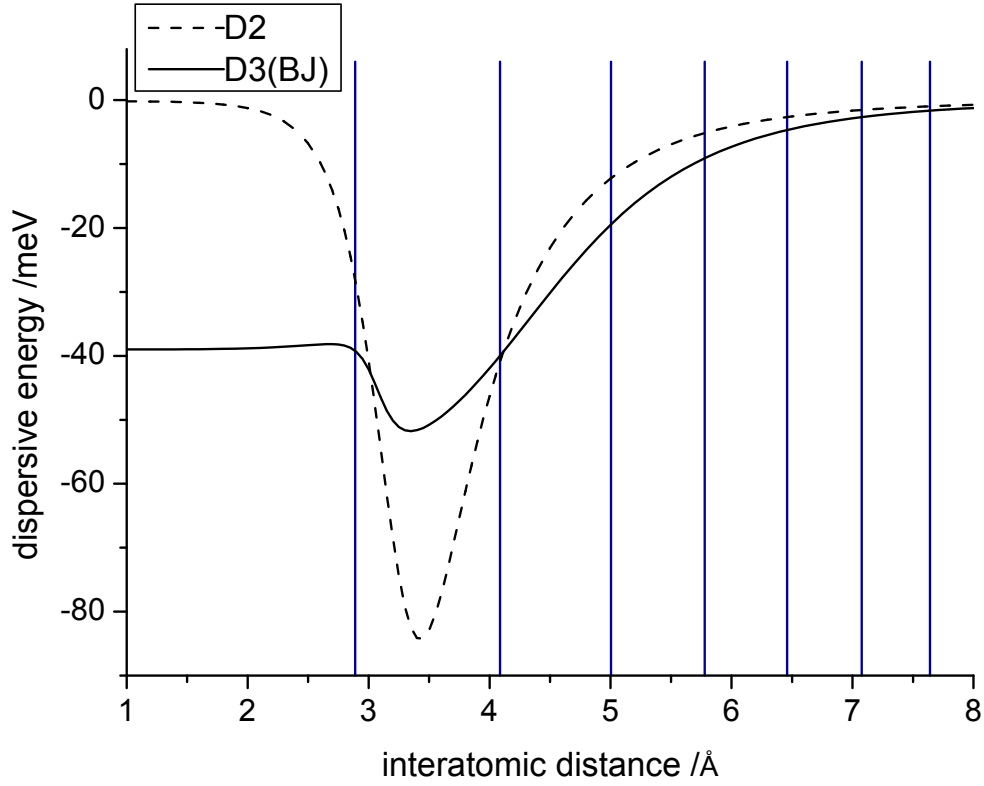


FIG. 3. D2- and D3(BJ)-Dispersion contributions between two silver atoms as a function of the inter atomic distance. The blue vertical lines indicate (from left to right) the experimental next neighbour, second next neighbour, etc. distances in the bulk silver structure.

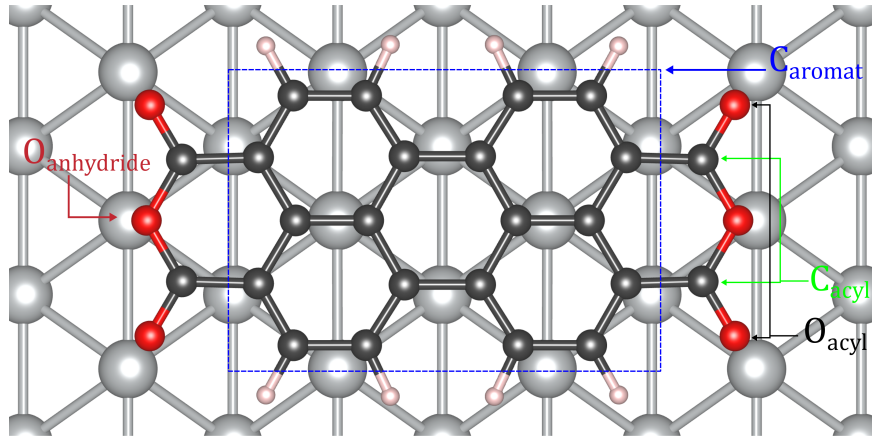


FIG. 4. PTCDA molecule on the Ag(110) surface; the perylene core is represented as the  $C_{\text{aronat}}$ , the acyl carbon atoms are marked as  $C_{\text{acyl}}$ , the anhydride oxygen as  $O_{\text{anhydride}}$  and the acyl oxygen as  $O_{\text{acyl}}$ .

TABLE II. XSW distances of the Ag170 cluster for different dispersion corrections as obtained with the fix12 scheme and the def2-TZVP basis. Distances are given in Å.

dispersion scheme	O <sub>acyl</sub>	O <sub>anhydride</sub>	C <sub>acyl</sub>	C <sub>aromat</sub>
noD	2.25	2.35	2.44	2.72
D2	2.28	2.37	2.43	2.67
D3(BJ)	2.31	2.41	2.47	2.64
slab D3(BJ) <sup>a</sup>	2.35	2.45	2.51	2.64
slab D3(BJ) <sup>b</sup>	2.38	2.46	2.53	2.71
expt. <sup>c</sup>	2.32	2.41	2.45	2.59

<sup>a</sup> this work

<sup>b</sup> Ref. [24]

<sup>c</sup> Ref. [12]

core (see Fig. 1) while C<sub>acyl</sub>, O<sub>anhydride</sub>, and O<sub>acyl</sub> denote the distances of the respective carbon and oxygen atoms (see Figs. 2 and 4).

In Table II we present the effect of changing the dispersion correction scheme. XSW distances of the Ag170 cluster are compared with the slab results of this work and of Ref. [24] as well as with the experimental results of Bauer *et al.* [12]. As also pointed out in prior work [22, 42–44] a proper inclusion of the dispersion interaction is of crucial importance for predicting a reliable structure for organic molecules upon a metal surface. Neglect of the dispersion interaction leads to much too short XSW distances of the oxygen atoms (about 0.07 Å shorter than the experimental values) while for the aromatic carbon atoms the corresponding values of the cluster are 0.11 Å larger than the experimental ones. Thus, if dispersion interaction is not taken into account, the organic molecule is predicted to be substantially buckled upon the surface due to covalent and ionic bonds between the metal and the electronegative oxygen atoms [12]. This buckling is diminished by dispersion interactions which provide a bonding mechanism between the carbon and silver atoms. Thus, while dispersion is not necessarily improving the description of the metal surface structure, it is mandatory for a realistic representation of the organic substrate upon the metal surface.

As already seen for the metal structure, Tab. II shows that the structure of PTCDA on the metal is better predicted by the more advanced D3(BJ) scheme than by its predecessor

TABLE III. XSW distances in Å upon variation of border fixing schemes for two different cluster models obtained with the def2-TZVP basis and the slab results. The D3(BJ) dispersion correction was used in all calculations.

cluster	fix status	O <sub>acyl</sub>	O <sub>anhydride</sub>	C <sub>acyl</sub>	C <sub>aromat</sub>
170	fix2	2.33	2.43	2.48	2.64
	fix12	2.31	2.41	2.47	2.64
290	fix2	2.34	2.44	2.49	2.62
	fix12	2.33	2.44	2.48	2.62

<sup>a</sup> this work

<sup>b</sup> Ref. [24]

<sup>c</sup> Ref. [12]

D2. The latter tends to underestimate the XSW distances of the oxygen atoms by 0.04 Å while the corresponding values for the aromatic carbon atoms are predicted to be 0.07 Å larger than the experimental values. In general the D2 dispersion correction performs better than the pure PBE approach but the D3(BJ) results are significantly better. Thus, we shall only discuss the latter in the following.

Keeping all other parameters fixed and varying the border fixing scheme for the 170 atom cluster (Ag170) we see that the fix2 (fixing the border atoms only in the second layer) scheme provides slightly larger XSW values than the fix12 (fixing the border atoms of the first and second layers) scheme (Table III). For the Ag170 cluster a change from the fix2 to the fix12 scheme causes an increase of all XSW values by 0.007–0.018 Å while for the biggest cluster, Ag290, the different schemes of fixing the border atoms has an almost negligible effect ( $< 0.003$  Å) on the XSW distances (Table III). In the following, we choose the fix12 scheme as the atoms far away from the molecule will not show significant displacement from their bare surface like positions.

In Table IV the XSW results for different basis sets and the Ag170 cluster are shown. With the def-SV(P) basis, the XSW distances of the acyl carbon and oxygen and for the anhydride oxygen – the functional atoms – are in good agreement (within 0.03 Å) with the slab-supercell approach but the deviation of the aromatic carbon is appreciably larger (0.09 Å). A much more balanced structure is obtained with the def2-TZVP basis which underestimates the

TABLE IV. XSW distances obtained for the Ag170 cluster and various basis sets. The fix12 scheme and the D3(BJ) dispersion correction were used for the cluster calculations. Distances are given in Å.

basis set	O <sub>acyl</sub>	O <sub>anhydride</sub>	C <sub>acyl</sub>	C <sub>aromat</sub>
def-SV(P)	2.38	2.45	2.54	2.73
def2-TZVP	2.31	2.41	2.47	2.64
partly def2-QZVP <sup>a</sup>	2.29	2.39	2.45	2.63
slab <sup>b</sup>	2.35	2.45	2.51	2.64

<sup>a</sup> def2-QZVP basis for PTCDA and first Ag layer atoms. def2-TZVP for other atoms.

<sup>b</sup> this work

XSW distances of the functional atoms by 0.03–0.04 Å but exactly reproduces the positions of the aromatic carbon atoms. This shows that the def2-TZVP is, as expected, a preferred choice over the def-SV(P) basis. With the larger mixed basis (partly def2-QZVP) all XSW distances decrease by 0.01–0.02 Å. All our results presented henceforth are performed with the def2-TZVP basis, which represents a good compromise between accuracy and efficiency.

In Tab. V, the XSW distances obtained for different cluster sizes with the def2-TZVP basis, the fix12 border atom fixing and the D3(BJ) dispersion correction are collected together with periodic slab and experimental results. The trend of the XSW distances of the respective atoms  $O_{acyl} < O_{anhydride} < C_{acyl} < C_{aromat}$  is obtained from the periodic calculations and for all clusters shown in Tab. V. However, this trend is not reproduced in all cases. In particular, the D2 dispersion scheme provides erratic substrate structures if small cluster sizes are employed (see supporting information for further details).

We see that the XSW distances essentially converge to the periodic results as the size of the clusters increase. The XSW distances of the Ag170 cluster are in significantly better agreement with the slab-supercell results if compared with the Ag32, Ag50 and Ag82 clusters. However, the XSW distances of this cluster are by about 0.03 Å shorter than the corresponding slab values. Increasing the cluster size tends to increase the XSW distances to the oxygen and the C<sub>acyl</sub> atoms while the C<sub>aromat</sub> distances decrease. We note that the change of these distances is not a smooth function of the number of atoms in the cluster as the Ag226 cluster predicts XSW distances that are about by 0.03 Å larger than the

TABLE V. XSW distances obtained for different cluster sizes, slab models and experimental data. The fix12 scheme, the def2-TZVP basis and the D3(BJ) dispersion correction was used for the cluster calculations. Distances are given in Å, adsorption energies,  $E_{\text{ads}}$ , in eV. The numbers in brackets are published error estimates.

cluster size	O <sub>acyl</sub>	O <sub>anhydride</sub>	C <sub>acyl</sub>	C <sub>aromat</sub>	$E_{\text{ads}}$
32	2.37	2.57	2.54	2.64	−4.5
50	2.42	2.58	2.56	2.62	−4.3
82	2.42	2.59	2.56	2.60	−4.2
170	2.31	2.41	2.47	2.64	−4.4
218	2.31	2.43	2.47	2.61	−4.4
226	2.36	2.45	2.50	2.63	−4.3
290	2.33	2.44	2.48	2.62	−4.5
slab <sup>a</sup>	2.35	2.45	2.51	2.64	−4.9
slab <sup>b</sup>	2.38	2.46	2.53	2.71	−4.4 <sup>c</sup>
expt. <sup>b</sup>	2.30(4)	2.38(3)	2.45(11)	2.58(1)	
expt. <sup>d</sup>	2.32(5)	2.41(6)	2.45(11)	2.59(1)	

<sup>a</sup> this work

<sup>b</sup> Ref. [12]

<sup>c</sup> estimated from Fig. 4 in Ref. [12]

<sup>d</sup> Ref. [24]

corresponding values of the Ag170, Ag218 and Ag290 clusters.

For the larger clusters (consisting of 170, 218, 226 and 290 Ag atoms) with D3(BJ) dispersion correction and def2-TZVP basis, the cluster results deviate only up to 0.03 Å from the periodic slab-supercell approach of the present work while the theoretical results of Bauer *et al.* [12] provide XSW distances which are 0.03–0.09 Å larger. We deduce that a metallic cluster should be able to retain properties of a true adsorbate molecule upon a metal surface if the metal cluster contains at least one row of metal atoms in lateral extension beyond the atoms that are in direct contact to the adsorbate molecule. However, the cluster approach itself represents an error source that limits the accuracy of the determined structure. For the larger cluster models the magnitude of these variations is smaller than uncertainties due

to the electronic structure method, the dispersion correction, or the basis set.

The computed adsorption energies are also displayed in Tab. V. The convergence of the cluster adsorption energies with the cluster size is comparable to the convergence of the XSW distances. A value of  $-4.4 \pm 0.1$  eV can be deduced from the variation of the adsorption energy for the clusters with 170 and more silver atoms. While this is in perfect agreement with the periodic slab results of Bauer *et al.* [12] our own slab calculations provide a lower adsorption energy of  $-4.90$  eV. Since our computational parameters are very similar to Ref.[12], this discrepancy requires further investigation.

#### IV. CONCLUSIONS AND OUTLOOK

We have investigated the applicability of the cluster approach for predicting the adsorbate structure of an organic molecule upon metallic surfaces. PTCDA on the Ag(110) surface was chosen for this comparison as it is experimentally well investigated and the standard theoretical approach (periodic slab supercell calculations) has been applied to this system. We chose to describe the electronic structure at the DFT level with the PBE functional.

Our results demonstrate that a reliable description of the surface substrate interaction requires several points to be addressed

- Dispersion interactions have to be added to the DFT approach preferably with the D3(BJ) [40] scheme which was found to be significantly better than the older D2 [37] variant. The latter tends to give rise to artificial surface reconstruction due to the damping of the dispersion interaction for short atomic distances which are ameliorated in the D3(BJ) approach.
- For the cluster approach sufficiently large basis sets are needed to converge the adsorbate properties. We found that the Ahlrichs triple- $\zeta$  quality basis set def2-TZVP is necessary for structural convergence within 0.02 Å.
- A consistent setup of the metal cluster turns out to be a nontrivial task. We deduce that a metallic cluster should be able to retain properties of a true adsorbate molecule upon a metal surface if the metal cluster contains at least one row of metal atoms in the lateral extension beyond the atoms that are in direct contact to the adsorbate molecule and a sufficient number of metal atom layers. Furthermore, during structure



optimisations it is important to fix the positions of atoms at the border of the cluster to their positions at the metal surface.

- Several “tricks” are required to make the cluster calculations feasible. Among them are the RI [55, 71] and MARI-J [56] approximations to accelerate the computations, a Fermi smearing to simplify the determination of occupations of orbitals near to the Fermi energy and appropriate damping schemes for the slowly converging SCF iterations.

The cluster approach provides a converged adsorption energy of PTCDA on Ag(110) of  $-4.4 \pm 0.1$  eV for the given DFT and dispersion method and the XSW distances of PTCDA on Ag(110) were determined with an accuracy of about 0.03 Å. The XSW distances of the larger clusters agree with those of the periodic slab calculations within this error limit. The variation of results from the cluster model indicate a limitation of this approach even for rather large cluster sizes. However, the “cluster-error” for XSW distances is in the same order of magnitude as experimental errors ( $\approx 0.05$  Å [82]) and smaller than the mean absolute error of 0.06 Å reported for the difference between theoretical and experimental XSW distances in the very recent work of Maurer *et al.* [25].

The present work indicates that it may be possible to design cluster methods that predict structural properties of organic adsorbates upon metal surfaces with a similar accuracy as experimental results. Such a protocol would be very useful as a computationally comparable or even favourable alternative to the well established periodic slab approach. This would have particular advantages for cases where periodic symmetry is absent due to the structure of the investigated system or for other cases where the periodic slab approach is not applicable. Last but not least, a validated finite cluster ansatz would provide an independent theoretical access to organic adsorbates on metal surfaces.

## V. ACKNOWLEDGEMENTS

We acknowledge support by the Volkswagen-Stiftung (BE and RFF) and the Deutsche Forschungsgemeinschaft DFG in the framework of the Research Training Group 1221 “Control of the Electronic Properties of Aggregated  $\pi$ -conjugated Molecules” (VS and BE) as well as the research project Fi620/3-1 (RFF and HGM) and the SFB 1083 “Structure and

Dynamics of Internal Interfaces” (RT). We are grateful for compute resources of the Centre for Light-Matter Interaction, Sensors & Analytics (LISA+) of the University of Tübingen and the HLR Stuttgart.

---

- [1] J. Scott and G. G. Malliaras, Chem. Phys. Lett., **299**, 115 (1999), ISSN 0009-2614.
- [2] S. R. Forrest, Nature, **428**, 911 (2004), ISSN 0028-0836.
- [3] J. C. Scott, J. Vacuum Sci. Technol. A, **21**, 521 (2003).
- [4] C. Santato and F. Rosei, Nature Chem., **2**, 344 (2010), ISSN 1755-4330.
- [5] S. Duhm, A. Gerlach, I. Salzmann, B. Bröker, R. Johnson, F. Schreiber, and N. Koch, Organic Electronics, **9**, 111 (2008), ISSN 1566-1199.
- [6] T.-C. Tseng, C. Urban, Y. Wang, R. Otero, S. L. Tait, M. Alcamí, D. Écija, M. Trelka, J. M. Gallego, N. Lin, M. Konuma, U. Starke, A. Nefedov, A. Langner, C. Woell, M. A. Herranz, F. Martín, N. Martín, K. Kern, and R. Miranda, Nature Chem., **2**, 374 (2010), ISSN 1755-4330.
- [7] S. Braun, W. R. Salaneck, and M. Fahlman, Adv. Mater., **21**, 1450 (2009), ISSN 1521-4095.
- [8] N. Watkins, L. Yan, and Y. Gao, Appl. Phys. Lett., **80**, 4384 (2002), ISSN 0003-6951.
- [9] S. Duhm, S. Hosoumi, I. Salzmann, A. Gerlach, M. Oehzelt, B. Wedl, T.-L. Lee, F. Schreiber, N. Koch, N. Ueno, and S. Kera, Phys. Rev. B, **81**, 045418 (2010).
- [10] A. Gerlach, S. Sellner, F. Schreiber, N. Koch, and J. Zegenhagen, Phys. Rev. B, **75**, 045401 (2007).
- [11] F. Tautz, Progr. Surf. Sci., **82**, 479 (2007), ISSN 0079-6816.
- [12] O. Bauer, G. Mercurio, M. Willenbockel, W. Reckien, C. Heinrich Schmitz, B. Fiedler, S. Soubatch, T. Bredow, F. S. Tautz, and M. Sokolowski, Phys. Rev. B, **86**, 235431 (2012).
- [13] A. C. Dürr, N. Koch, M. Kelsch, A. Rühm, J. Ghijsen, R. L. Johnson, J.-J. Pireaux, J. Schwartz, F. Schreiber, H. Dosch, and A. Kahn, Phys. Rev. B, **68**, 115428 (2003).
- [14] C. Bürker, N. Ferri, A. Tkatchenko, A. Gerlach, J. Niederhausen, T. Hosokai, S. Duhm, J. Zegenhagen, N. Koch, and F. Schreiber, Phys. Rev. B, **87**, 165443 (2013).
- [15] A. Gerlach, F. Schreiber, S. Sellner, H. Dosch, I. A. Vartanyants, B. C. C. Cowie, T.-L. Lee, and J. Zegenhagen, Phys. Rev. B, **71**, 205425 (2005).
- [16] Y. Y. Zhang, S. X. Du, and H.-J. Gao, Phys. Rev. B, **84**, 125446 (2011).

- [17] R. Temirov, S. Soubatch, A. Luican, and F. S. Tautz, *Nature*, **444**, 350 (2006), ISSN 0028-0836.
- [18] A. Alkauskas, A. Baratoff, and C. Bruder, *Phys. Rev. B*, **73**, 165408 (2006).
- [19] F. S. Tautz, S. Sloboshanin, J. A. Schaefer, R. Scholz, V. Shklover, M. Sokolowski, and E. Umbach, *Phys. Rev. B*, **61**, 16933 (2000).
- [20] M. Wießner, D. Hauschild, A. Schöll, F. Reinert, V. Feyer, K. Winkler, and B. Krömker, *Phys. Rev. B*, **86**, 045417 (2012).
- [21] J. Ziroff, F. Forster, A. Schöll, P. Puschnig, and F. Reinert, *Phys. Rev. Lett.*, **104**, 233004 (2010).
- [22] A. Abbasi and R. Scholz, *J. Phys. Chem. C*, **113**, 19897 (2009), <http://pubs.acs.org/doi/pdf/10.1021/jp902370b>.
- [23] Y. Zou, L. Kilian, A. Schöll, T. Schmidt, R. Fink, and E. Umbach, *Surf. Sci.*, **600**, 1240 (2006), ISSN 0039-6028.
- [24] G. Mercurio, O. Bauer, M. Willenbockel, N. Fairley, W. Reckien, C. H. Schmitz, B. Fiedler, S. Soubatch, T. Bredow, M. Sokolowski, and F. S. Tautz, *Phys. Rev. B*, **87**, 045421 (2013).
- [25] R. J. Maurer, V. G. Ruiz, J. Camarillo-Cisneros, W. Liu, N. Ferri, K. Reuter, and A. Tkatchenko, *Progress in Surface Science*, **91**, 72 (2016), ISSN 0079-6816.
- [26] P. Hohenberg and W. Kohn, *Phys. Rev.*, **136**, B864 (1964).
- [27] W. Kohn and L. J. Sham, *Phys. Rev.*, **137**, A1697 (1965).
- [28] E. Gross and W. Kohn, *Phys. Rev. Lett.*, **55**, 2850 (1985).
- [29] M. E. Casida, C. Jamorski, K. C. Casida, and D. R. Salahub, *J. Chem. Phys.*, **108**, 4439 (1998).
- [30] T. A. Wesolowski, P.-Y. Morgantini, and J. Weber, *J. Chem. Phys.*, **116**, 6411 (2002).
- [31] J. P. Perdew and Y. Wang, *Phys. Rev. B*, **45**, 13244 (1992).
- [32] J. P. Perdew, K. Burke, and M. Ernzerhof, *Phys. Rev. Lett.*, **77**, 3865 (1996).
- [33] D. C. Langreth and M. J. Mehl, *Phys. Rev. B*, **28**, 1809 (1983).
- [34] A. Tkatchenko and M. Scheffler, *Phys. Rev. Lett.*, **102**, 073005 (2009).
- [35] V. G. Ruiz, W. Liu, E. Zofer, M. Scheffler, and A. Tkatchenko, *Phys. Rev. Lett.*, **108**, 146103 (2012).
- [36] S. Grimme, *J. Comput. Chem.*, **25**, 1463 (2004), ISSN 1096-987X.
- [37] S. Grimme, *J. Comput. Chem.*, **27**, 1787 (2006), ISSN 1096-987X.

- [38] S. Grimme, J. Antony, S. Ehrlich, and H. Krieg, *J. Chem. Phys.*, **132**, 154104 (2010).
- [39] S. Grimme, *Wiley Interdisciplinary Reviews: Computational Molecular Science*, **1**, 211 (2011), ISSN 1759-0884.
- [40] S. Grimme, S. Ehrlich, and L. Goerigk, *J. Comput. Chem.*, **32**, 1456 (2011), ISSN 1096-987X.
- [41] R. Caputo, B. P. Prascher, V. Staemmler, P. S. Bagus, and C. Wöll, *J. Phys. Chem. A*, **111**, 12778 (2007), pMID: 17999480, <http://pubs.acs.org/doi/pdf/10.1021/jp076339q>.
- [42] A. Tkatchenko, L. Romaner, O. T. Hofmann, E. Zojer, C. Ambrosch-Draxl, and M. Scheffler, *MRS Bulletin*, **35**, 435 (2010).
- [43] R. Scholz and A. Abbasi, *Physica Status Solidi C*, **7**, 236 (2010), ISSN 1610-1642.
- [44] P. Sony, P. Puschnig, D. Nabok, and C. Ambrosch-Draxl, *Phys. Rev. Lett.*, **99**, 176401 (2007).
- [45] R. Tonner, P. Rosenow, and P. Jakob, *Phys. Chem. Chem. Phys.*, **18**, 6316 (2016).
- [46] P. Puschnig, E.-M. Reinisch, T. Ules, G. Koller, S. Soubatch, M. Ostler, L. Romaner, F. S. Tautz, C. Ambrosch-Draxl, and M. G. Ramsey, *Phys. Rev. B*, **84**, 235427 (2011).
- [47] W.-L. Yim and T. Klüner, *Phys. Rev. Lett.*, **110**, 196101 (2013).
- [48] V. Staemmler, in *Theoretical Aspects of Transition Metal Catalysis*, Topics in Organometallic Chemistry, Vol. 12, edited by G. Frenking (Springer Berlin Heidelberg, 2005) pp. 219–256, ISBN 978-3-540-23510-1.
- [49] T. Jacob and W. A. Goddard, *ChemPhysChem*, **7**, 992 (2006), ISSN 1439-7641.
- [50] P. S. Bagus, A. Wieckowski, and C. Wöll, *Int. J. Quant. Chem.*, **110**, 2844 (2010), ISSN 1097-461X.
- [51] M. Kettner, W. B. Schneider, and A. A. Auer, *J. Phys. Chem. C*, **116**, 15432 (2012), <http://dx.doi.org/10.1021/jp303773y>.
- [52] W. B. Schneider, U. Benedikt, and A. A. Auer, *ChemPhysChem*, **14**, 2984 (2013), ISSN 1439-7641.
- [53] S. Nigam and C. Majumder, *Surf. Sci.*, **630**, 78 (2014), ISSN 0039-6028.
- [54] J. Hafner, *J. Comput. Chem.*, **29**, 2044 (2008), ISSN 1096-987X.
- [55] K. Eichkorn, F. Weigend, O. Treutler, and R. Ahlrichs, *Theoret. Chem. Acc.*, **97**, 119 (1997), ISSN 1432-881X.
- [56] M. Sierka, A. Hogekamp, and R. Ahlrichs, *J. Chem. Phys.*, **118**, 9136 (2003).
- [57] A. D. Rabuck and G. E. Scuseria, *J. Chem. Phys.*, **110**, 695 (1999).

- [58] A. D. Becke and E. R. Johnson, J. Chem. Phys., **127**, 154108 (2007), doi:  
<http://dx.doi.org/10.1063/1.2795701>.
- [59] G. Kresse and J. Hafner, Phys. Rev. B, **47**, 558 (1993).
- [60] G. Kresse and J. Hafner, Phys. Rev. B, **49**, 14251 (1994).
- [61] G. Kresse and J. Furthmüller, Phys. Rev. B, **54**, 11169 (1996).
- [62] G. Kresse and J. Furthmüller, Computational Materials Science, **6**, 15 (1996), ISSN 0927-0256.
- [63] M. Methfessel and A. T. Paxton, Phys. Rev. B, **40**, 3616 (1989).
- [64] H. J. Monkhorst and J. D. Pack, Phys. Rev. B, **13**, 5188 (1976).
- [65] K. Glöckler, C. Seidel, A. Soukopp, M. Sokolowski, E. Umbach, M. Böhringer, R. Berndt, and W.-D. Schneider, Surf. Sci., **405**, 1 (1998), ISSN 0039-6028.
- [66] M. Böhringer, W.-D. Schneider, K. Glöckler, E. Umbach, and R. Berndt, Surf. Sci., **419**, L95 (1998), ISSN 0039-6028.
- [67] “TURBOMOLE V6.5 2013, a development of University of Karlsruhe and Forschungszentrum Karlsruhe GmbH, 1989-2007, TURBOMOLE GmbH, since 2007; available from <http://www.turbomole.com>.” (2013).
- [68] R. Ahlrichs, M. Bär, M. Häser, H. Horn, and C. Kölmel, Chem. Phys. Lett., **162**, 165 (1989), ISSN 0009-2614.
- [69] M. Von Arnim and R. Ahlrichs, J. Comput. Chem., **19**, 1746 (1998), ISSN 1096-987X.
- [70] K. Eichkorn, O. Treutler, H. Öhm, M. Häser, and R. Ahlrichs, Chem. Phys. Lett., **240**, 283 (1995), ISSN 0009-2614.
- [71] O. Vahtras, J. Almlöf, and M. W. Feyereisen, Chem. Phys. Lett., **213**, 514 (1993).
- [72] A. Schafer, H. Horn, and R. Ahlrichs, J. Chem. Phys., **97**, 2571 (1992).
- [73] F. Weigend and R. Ahlrichs, Phys. Chem. Chem. Phys., **7**, 3297 (2005).
- [74] F. Weigend, Phys. Chem. Chem. Phys., **8**, 1057 (2006).
- [75] D. Andrae, U. Häußermann, M. Dolg, H. Stoll, and H. Preuß, Theoret. Chem. Acc., **77**, 123 (1990), ISSN 1432-881X, 10.1007/BF01114537.
- [76] P.-A. Malmqvist, J. Olsen, P. R. Taylor, J. Almlöv, R. Ahlrichs, and P. E. M. Siegbahn, in *European Summerschool in Quantum Chemistry, Book I*, edited by B. Roos and P.-O. Widmark (University of Lund, 1999).
- [77] D. P. Woodruff, Rep. Prog. Phys., **68**, 743 (2005).

- [78] “Lattice constants of the elements,” <http://periodictable.com/Properties/A/LatticeConstants.html>, accessed: 2016-09-20.
- [79] V. B. Nascimento, E. A. Soares, V. E. de Carvalho, E. L. Lopes, R. Paniago, and C. M. C. de Castilho, Phys. Rev. B, **68**, 245408 (2003).
- [80] Y. Wang, W. Wang, K.-N. Fan, and J. Deng, Surf. Sci., **490**, 125 (2001), ISSN 0039-6028.
- [81] S. Narasimhan, Surf. Sci., **496**, 331 (2002), ISSN 0039-6028.
- [82] A. Gerlach and F. Schreiber, in *Handbook of Spectroscopy*, edited by G. Gauglitz and D. S. Moore (Wiley-VCH, Weinheim, 2014) p. 1507.